

*On the Combustion Characteristics of a Novel Biofuel: Heat of Combustion and Vaporization Rate

M. Birouk¹, A. I. Chowdhury¹, D. Levin², M. Sailer³, J. Sorensen³

¹Department of Mechanical Engineering, University of Manitoba, Winnipeg, MB, Canada

²Department of Biosystems Engineering, University of Manitoba, Winnipeg, MB, Canada

³Department of Chemistry, University of Manitoba, Winnipeg, MB, Canada

1 Introduction

The global economy is highly dependent on petroleum, and although the cost of petroleum is currently low, long-term forecasts indicate that fossil fuel costs will increase significantly as “sweet crude” reserves dwindle, and lower quality reserves that are in more remote, inaccessible, and/or environmentally sensitive locations are developed. By 2050, the global population is expected to reach 9 billion, and energy consumption will increase by 52%, due to rapid industrialization, growth in transportation, electricity generation, agricultural sector and other basic human needs, all of which contribute to environmental degradation. In addition, the reserves of Petroleum-based fuels are concentrated in certain geopolitically sensitive regions of the world. Together these facts are driving a global effort to develop renewable energy sources.

It was reported that, to date, about 16% of global energy consumption comes from renewable resources (e.g., [1-3]). The slow progress in the development and implementation of renewable energy sources is mainly attributed to several factors such as economic limitations, lack of supply, and technical know-how of users (e.g., [4]). Renewable energy sources can be categorized into two groups; the first consists of clean energy technologies such as, solar, wind, hydroelectric, wave and rain energy; while the second one consists of biofuel technologies derived from renewable biomass. Renewable biofuels, such as bioethanol and biodiesel, can be used to displace consumption of petroleum-derived diesel and gasoline in transportation and offer the potential for growth in the direction of sustainable mobility with the involvement of the energy, agricultural, automotive, and aerospace transportation sectors.

Biodiesel fuels are composed of mono-alkyl esters of long chain fatty acids produced from biomass such as agricultural oil seed crops, animal fats, and other non-edible oil sources (e.g., [5-7]). Biodiesel is commonly used in compression ignition engines as an additive with fossil derived diesel fuel. It has various advantages such as higher flash point and cetane number; lower toxicity; lower emissions of particulates; better lubricity and safety (e.g., [8-10]). For instance, biodiesel can offer other benefits, including reduction of greenhouse gas by emitting fewer pollutants over the whole range of air–fuel ratio when compared to diesel (e.g., [11]). In spite of the above advantages, drawbacks, such as reduced cold flow property, higher pour point and cloud point [12-14], lower oxidation stability, storage and thermal instability, higher crystallization temperatures [9, 15], higher viscosity,

* This research was funded by BioFuelNet Canada

lower energy content, and higher price [16], have restricted the application of biodiesel as the fuel for diesel engines. For instance, biodiesel derived from fats or oils with significant amounts of saturated fatty compounds have undesirable fuel properties that limit their applications in cold weather conditions [17]. Improvement of the low temperature flow characteristic still remains one of the major challenges when using biodiesel as an alternative fuel for diesel engines. Several methods have been suggested to improve biodiesel characteristics at lower temperature, such as blending with petroleum fuel, vegetable oil methyl esters (e.g., [12, 18-19]), or using additives (e.g., methanol, ethanol, kerosene) [20-22]).

The main objective of the present research was to develop and test a novel bio-based liquid substance as an additive for improving cold flow performance of biodiesel, or as stand-alone fuel. We chose to use 1,3-dimethoxyoctane as a novel fuel/fuel additive. The 1,3-dimethoxyoctane used in this study was prepared from methyl 3-hydroxyoctanoate as described in Section 2. Some combustion properties such as the vaporization rate and heat of combustion were measured and compared with established fuels to assess the merit of the newly developed biofuel/fuel additive.

2 Material and Fuel Production

The substrate, methyl 3-hydroxyoctanoate was reduced with sodium borohydride (NaBH_4 ; 2.5 equivalents) in THF overnight at room temperature to produce 1,3-octanediol, after acidic workup, in good yield. The 1,3-octanediol was purified with column chromatography over silica gel and used as a substrate for the next step. A solution of 1,3-octanediol in THF was reacted with 1.5 equivalents of sodium hydride (NaH) at room temperature for 15 min, after which time 3 equivalents of methyl iodide (CH_3I) were added and the reaction allowed to stir at room temperature overnight. The reaction was quenched by the addition of sodium hydroxide solution, followed by a washing of the organic layer with water. The 1,3-dimethoxyoctane was dried with Na_2SO_4 , and the solids were removed by filtration. The 1,3-dimethoxyoctane (called thereafter 1,3-DMO) produced by this method was > 95% pure as determined by $^1\text{H-NMR}$ and was used directly in combustion testing.

3 Experimental Tests

The in-house experimental tests to determine the heat of combustion (that is, the lower heat value (LHV)) and the vaporization rate of the newly developed biofuel/fuel additive 1,3-DMO, were conducted using test rigs described briefly below.

3.1. Droplet vaporization: The experimental setup used for testing the fuel evaporation consisted of a spherical combustion chamber/vessel with a capacity of about 30 liters. This set up was described elsewhere [23-25], and thus only a brief description is provided here. It is designed to generate isotropic and homogeneous turbulence under elevated pressure and temperature conditions which make it possible to vary turbulent Reynolds number as well as turbulent length scales. The turbulent flow-field is generated by four pairs of axial opposed fans capable of spinning up to 6000 RPM. The spherical combustion chamber has two pairs of opposed optical/quartz windows positioned 90-degrees apart which are designed to enable visualization and imaging at atmospheric and elevated pressure and temperature conditions. The vessel can be pressurized using compressed nitrogen supplied from a compressed cylinder. The set pressure inside the vessel was controlled using a Cecom Electronics pressure gauge having an accuracy of $\pm 0.25\%$ of full scale. The nitrogen inside the vessel was heated using a 2-kW bank of Etirex heating elements and the set temperature was controlled using an Omega K-type thermocouple with an accuracy of $\pm 0.75\%$ of full scale [24-25]. A single droplet was formed using an in-house designed retractable injection system by pumping/discharging liquid fuel through a needle having an inner diameter of about 0.254 mm. The droplet was deposited onto the tip of a quartz filament suspended in the center of the vessel (i.e., [23-25]). A halogen lamp was used to backlit the droplet in order to enhance the contrast of its projected surface area. The temporal regression of the projected droplet surface area was captured using a Nanosence MKIII high speed CCD camera having a maximum of 1000 frames per second at full resolution of 1280 x 1024 pixels. An in-house developed Matlab code was used to determine the droplet projected surface area. The latter was calculated in pixels and converted into volume from which the droplet instantaneous

diameter was calculated. The error due to image processing was found to be less than $\pm 5\%$. At least three experiments were carried at each test condition, and the results were found repeatable to less than $\pm 5\%$. Two types of tests were performed; one in quiescent atmospheric pressure by varying the ambient temperature from room temperature up to 448 K, and the other by varying the turbulence intensity via increasing the fan blades speed from zero up to 2000 rpm in a hot atmospheric environment (i.e., 1 atm, 423 K). The liquid fuel tested was 1,3-DMO.

3.2. Heat of Combustion: The experimental setup, which was used for determining the fuel heat of combustion (called also lower heating value (LHV)), consisted of a “bomb calorimeter” where the combustion occurs at high pressure. It is a sealed container designed to measure the heating value of liquid fuels. A carefully weighed sample of a substance (i.e., liquid fuel) is placed inside the bomb in contact with an igniter. The bomb is then filled up with oxygen to a pressure of about 30 bar, sealed, and placed into a known amount of water. Burning takes place by igniting the substance with an electric current which is passed through a wire. The heat released raises the temperature of the calorimeter and its surrounding water as the combustion takes place. The temperature rise is measured by a thermocouple. Three experiments were carried out for each sample, and the results were repeatable to less than $\pm 2\%$.

4 Results and Discussion

Comprehensive characterization of the turbulent flow field inside the combustion chamber was reported elsewhere [23-25]. Figure 1 shows the temporal variation of the normalized squared diameter of 1,3-DMO droplet at different ambient temperatures and standard atmospheric pressure. The majority of the time histories exhibit a linear variation where the d^2 -law holds perfectly. This scenario is similar at different ambient temperatures. However, the d^2 -law does not hold when the droplet is nearing its depletion where the evolution of d^2 departs from a linear variation. This is caused by the accumulation of the heaviest components of the fuel. In addition, Figure 1 shows a rapid reduction in the lifetime of the droplet with increasing ambient temperature indicating a strong dependence of the droplet vaporization upon the surrounding gas temperature. Figure 2 shows the normalized droplet vaporization rate versus the ambient temperature (where K and K_0 are, respectively, the droplet vaporization rate at different ambient temperatures and room temperature). In this figure, the data of at least three tests at each fixed ambient temperature are plotted. Published experimental data of decane droplet are also included in this figure, which were obtained at ambient temperatures ranging between room and 373 K [24]. This figure reveals that both 1,3-DMO and decane droplets exhibit similar trends within the ambient temperature range up to 373 K; however, the decane droplet exhibits a significantly lower vaporization rate. For instance, the vaporization rate of the 1,3-DMO droplet at 373 K increases by about 100 times versus that at room temperature; whereas it increases by only 50 times for decane droplet. Similar trends are observed at an ambient temperature of 323 K where the increase in K of the newly developed fuel is only 6 times and that of decane is 4 times. These results suggest that 1,3-DMO has a much stronger dependence on the ambient temperature where K/K_0 follows a very steep increases at ambient temperatures greater than 373 K. Table 2 shows also that the vaporization rate of 1,3-DMO, at 373 K, is only 3 times less than that of ethanol, gasoline and or decane. Figure 3 depicts the time histories of the 1,3-DMO droplet for different ambient turbulence levels at a constant ambient temperature, 423 K, and atmospheric pressure. The droplet time histories in quiescent atmosphere show a short heating period followed by a linear variation. However, no significant heating period is observed in the presence of a turbulent flow field as the $(d/d_0)^2$ varies linearly with time indicating the applicability of the classical d^2 -law. The same figure shows a significant decrease in the droplet lifetime as turbulence intensity increases. This is clearly shown in Figure 4, which presents the droplet normalized vaporization rate as a function of turbulence intensity (where K and K_0 are, respectively, the droplet vaporization rate at different turbulent intensity and quiescent environment). This figure shows that the droplet evaporation rate increases with turbulence intensity. This is in agreement with our previous findings on the effect of turbulence on the vaporization of hydrocarbon [24] and biodiesel [25] droplets where the effect turbulence was shown to exert a greater influence at low turbulence

levels indicating that the dominant role of turbulence is to diffuse the vapor away from the droplet surface. Additional data will be reported in the final manuscript to compare with biodiesel and decane as well as ethanol.

The heat of combustion was measured for the 1,3-DMO fuel using the calorimeter set-up described above. Three tests were conducted to ensure the accuracy and repeatability of the measurements. The tests results revealed that the heat of combustion of 1,3-DMO is 37.745 ± 0.11 MJ/kg, which is 47.87% and 28.99% higher than that of methanol and ethanol, respectively. However, the heat of combustion of the 1,3-DMO fuel is comparable to that of biodiesel; for example, it is only about 5% less than that of Canola biodiesel, and about 15% less than that of decane fuel, and only 11% less than that of petroleum diesel. A summary is provided in Table 1.

5 Conclusions

A novel liquid biofuel / fuel additive was developed and some preliminary tests were carried out. The results revealed that this novel biofuel has a lower heating value almost equal to that of pure biodiesel and approximately 50% greater than that of ethanol. However, this fuel was found to be much more volatile than biodiesel. The tests revealed that the vaporization rate of this fuel can be easily determined using the d^2 -law. Its vaporization rate is much higher than that of biodiesel fuel and only slightly lower than that of decane, gasoline or ethanol. These preliminary results suggest that this newly developed liquid biofuel may easily be used as standalone fuel.

References

- [1] Martinot E, Dienst C, Weiliang L, Qimin C. Renewable energy futures: targets, scenarios, and pathways. *Annu Rev Environ Resour* 2007; 32:205–39.”
- [2] Azad AK, Rasul MG, Khan MMK, Ahasan T, Ahmed SF. Energy scenario: production, consumption and prospect of renewable energy in Australia. *J Power Energy Eng* 2014; 2(4):19–25.
- [3] Lund H. Renewable energy strategies for sustainable development. *Energy* 2007; 32(6):912–9.
- [4] R. D. Misra and M. S. Murthy, Straight vegetable oils usage in a compression ignition engine—A review, *Renew. Sustain. Energy Rev.*, vol. 14, no. 9, pp. 3005–3013, Dec. 2010.
- [5] E. Kondili and J. Kaldellis, Biofuel implementation in East Europe: Current status and future prospects, *Renew. Sustain. Energy Rev.*, vol. 11, no. 9, pp. 2137–2151, Dec. 2007.
- [6] Sarin A, Arora R, Singh N, Sarin R, Malhotra R, Sarin S. Blends of biodiesels synthesized from non edible and edible oils: effects on the cold filter plugging point. *Energy Fuels* 2010; 24(3):1996–2001.
- [7] A. Demirbas, Progress and recent trends in biodiesel fuels, *Energy Convers. Manag.*, vol. 50, no. 1, pp. 14–34, Jan. 2009.
- [8] P. C. Smith, Y. Ngothai, Q. Dzuy Nguyen, and B. K. O’Neill, Improving the low-temperature properties of biodiesel: Methods and consequences, *Renew. Energy*, vol. 35, no. 6, pp. 1145–1151, Jun. 2010.
- [9] M. De Torres, G. Jiménez-Osés, J. a. Mayoral, and E. Pires, Fatty acid derivatives and their use as CFPP additives in biodiesel, *Bioresour. Technol.*, vol. 102, no. 3, pp. 2590–2594, Feb. 2011.
- [10] Misra, R. D., and M. S. Murthy. Blending of additives with biodiesels to improve the cold flow properties, combustion and emission performance in a compression ignition engine—A review.’ *Renewable and Sustainable Energy Reviews* 15.5 (2011): 2413-2422.
- [11] A. H. Demirbas and I. Demirbas, Importance of rural bioenergy for developing countries, *Energy Convers. Manag.*, vol. 48, no. 8, pp. 2386–2398, Aug. 2007. [12] R. Sarin, M. Sharma, S. Sinharay, and R. K. Malhotra, “Jatropha-Palm biodiesel blends: An optimum mix for Asia,” *Fuel*, vol. 86, no. 10–11, pp. 1365–1371, Jul. 2007.

- [13] Demirbas A. Biodiesel: a realistic fuel alternative for diesel engines. Springer; 2008.
- [14] C.-W. Chiu, L. G. Schumacher, and G. J. Suppes, Impact of cold flow improvers on soybean biodiesel blend, *Biomass and Bioenergy*, vol. 27, no. 5, pp. 485–491, Nov. 2004.
- [15] S. Jain and M. P. Sharma, Stability of biodiesel and its blends: A review, *Renew. Sustain. Energy Rev.*, vol. 14, no. 2, pp. 667–678, Feb. 2010.
- [16] Demirbas A. New liquid biofuels from vegetable oils via catalytic pyrolysis. *Energy Educ Sci Technol* 21:1–59, 2008.
- [17] G. Knothe, Designer' Biodiesel: Optimizing Fatty Ester Composition to Improve Fuel Properties, *Energy & Fuels*, vol. 22, no. 2, pp. 1358–1364, Mar. 2008.
- [18] B. R. Moser, Influence of Blending Canola, Palm, Soybean, and Sunflower Oil Methyl Esters on Fuel Properties of Biodiesel, *Energy Fuels*, 2008, 22 (6), pp 4301–4306.
- [19] C. Echim, J. Maes, and W. De Greyt, Improvement of cold filter plugging point of biodiesel from alternative feedstocks, *Fuel*, vol. 93, pp. 642–648, Mar. 2012.
- [20] Kazancev, Kiril, et al. Cold flow properties of fuel mixtures containing biodiesel derived from animal fatty waste, *European Journal of Lipid Science and Technology* 108.9 (2006): 753-758.
- [21] P. Udomsap, U. Sahapatsombat, B. Puttasawat, P. Krasae, N. Chollacoop, and S. Topaiboul, "Preliminary Investigation of Cold Flow Improvers for Palm-Derived Biodiesel Blends," vol. 18, no. 2, pp. 99–102, 2008.
- [22] Y. Wang, S. Ma, M. Zhao, L. Kuang, J. Nie, and W. W. Riley, Improving the cold flow properties of biodiesel from waste cooking oil by surfactants and detergent fractionation, *Fuel*, vol. 90, no. 3, pp. 1036–1040, 2011.
- [23] M. Birouk and S. C. Fabbro, Droplet evaporation in a turbulent atmosphere at elevated pressure – Experimental data, *Proc. Combust. Inst.*, vol. 34, no. 1, pp. 1577–1584, 2013.
- [24] Birouk, M. (2014) A hydrocarbon droplet evaporation in turbulent environment at elevated ambient pressure and temperature, *Combustion Science and Technology*, 176 (10-11), pp. 1295-1308.
- [25] Birouk, M. and Toth, S. (2015) Vaporization and combustion of soybean biodiesel droplet in turbulent environment at elevated ambient pressure, *Combustion Science and Technology*, Vol. 187(6), pp. 937-952.
- [26] D. H. Qi, H. Chen, L. M. Geng, Y. Z. Bian, and X. C. Ren, Performance and combustion characteristics of biodiesel–diesel–methanol blend fuelled engine, *Appl. Energy*, vol. 87, no. 5, pp. 1679–1686, 2010.
- [27] D. C. Rakopoulos, C. D. Rakopoulos, R. G. Papagiannakis, and D. C. Kyritsis, Combustion heat release analysis of ethanol or n-butanol diesel fuel blends in heavy-duty DI diesel engine, *Fuel*, vol. 90(5), pp. 1855–1867, 2011.
- [28] E. V Sagadeev, R. A. Kafiatullin, V. V Sagadeev, and V. I. Sagadeev, Applying an Additive Scheme to the Calculation of the Heat of Combustion of Saturated Hydrocarbons, vol. 37(1), pp. 100–103, 2003.
- [29] Kobayasi, K., A Study on the Evaporation Velocity of a Single Liquid Droplet. *Technol. Reports Tohoku University*, 18:209, 1954)

Table 1: Heat of combustion of the newly developed fuel/fuel additive and other fuels

Property	Methanol	Ethanol	1,3-DMO	Canola Biodiesel	Diesel	Decane
LHV (MJ/kg)	19.67 [26]	26.80 [27]	37.75	39.78	42.50 [26]	44.60 [28]
% increase or	- 47.87	- 28.99		+ 5.09	+ 11.18	+ 15.36

decrease in LHV					
-----------------	--	--	--	--	--

Table 2: Droplet vaporization rate of selected fuels at 373 K and 1 atm

Fuel	1,3-DMO	Ethanol	Gasoline	Decane
K [mm ² /s]	0.011	0.030 [29]	0.032 [29]	0.032 [24]

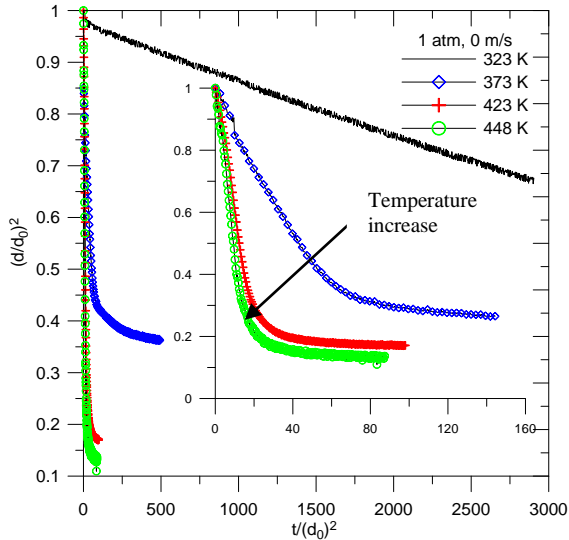


Figure 1: Time histories of the vaporization of 1,3-dimethoxyoctane droplet for different ambient temperatures at atmospheric pressure

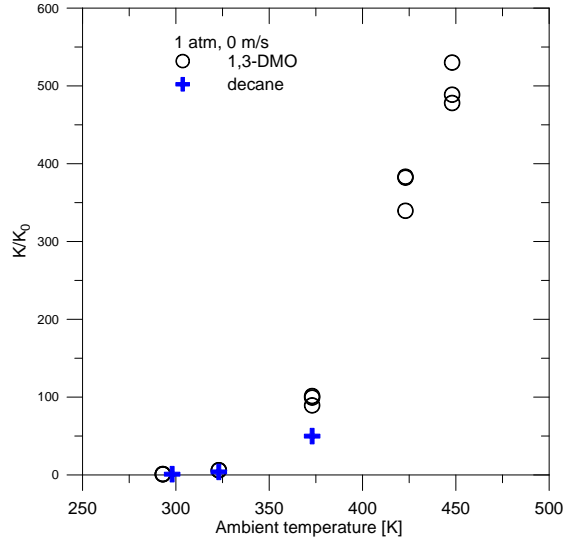


Figure 2: Normalized evaporation rate of 1,3-dimethoxyoctane droplet as a function of ambient temperature in quiescent atmosphere

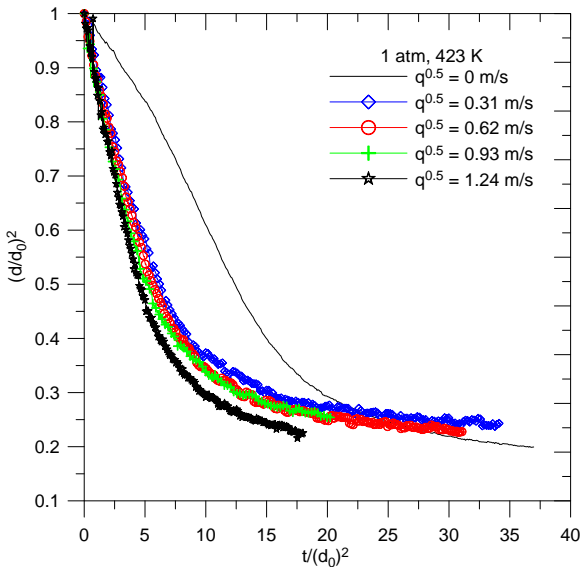


Figure 3: Time histories of the vaporization of 1,3-dimethoxyoctane droplet for different turbulence intensities at atmospheric ambient pressure and hot environment (423 K).

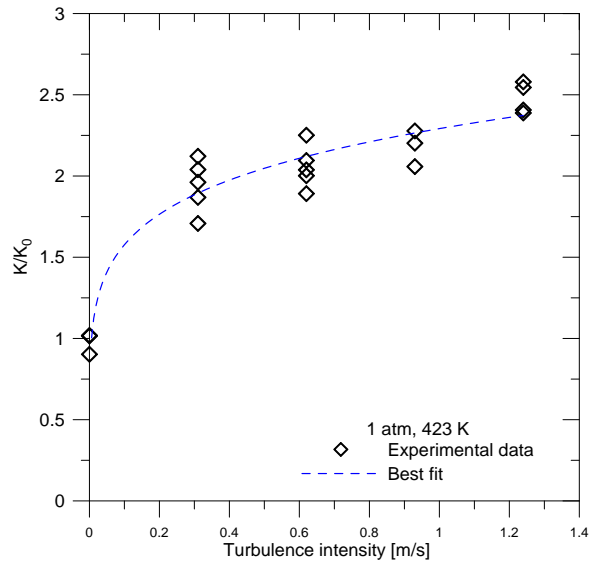


Figure 4: Normalized evaporation rate of 1,3-dimethoxyoctane droplet as a function of turbulence intensity at 1 atm and 423 K.